Universidade Nova de Lisboa
OMNIS CIVITAS CONTRA SE DIVISA NON STABIT

Faculdade de Ciência e Tecnologia, Departamento de Engenheria Civil

APPLICATION OF PUSHOVER ANALYSIS ON REINFORCED CONCRETE BRIDGE MODEL

Part II – CASE STUDY

Dr. Cosmin G. Chiorean

Post-doctoral fellowship, UNL/FCT-DEC

Research Report No. POCTI/36019/99

December 2003

1. DESCRIPTION OF STRUCTURE

A three span prestressed reinforced concrete bridge, which is to be built in the northeastern of Portugal over Alva River, is chosen as a case study. The total length of the bridge is 115 m with spans of 35, 45, and 35 m. Figure 1 shows the structural model of the bridge and the relevant cross-sectional types. The geometrical and mechanical characteristics of the bridge and the relevant cross-sections are presented in the technical plants in Appendix A. Also the profile of the prestressing cable and the effective prestressed force applied in superstructure of the bridge, are presented in appendix A

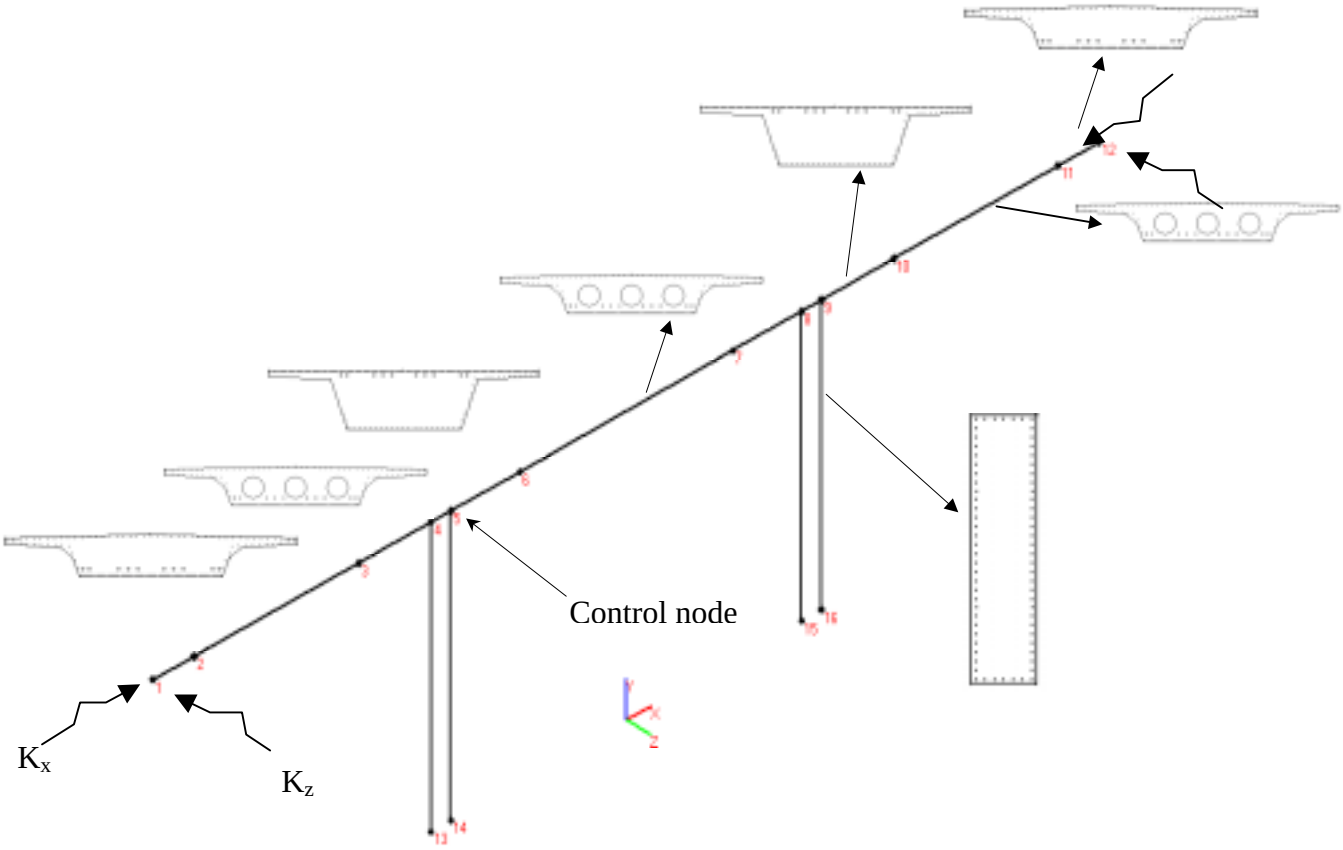

Figure 1. Structural model of the bridge

1.1 Numerical model

The nonlinear inelastic analysis program NEFCAD [6] was used as the base analytical platform for the study. Among the basic features that made NEFCAD suitable for this evaluation were: (i) distributed flexibility model to represent explicitly (fiber approach) and implicitly (M-N-Φ approach) spread of plasticity effects; (ii) large deflections and large rotations; (iii) linear and nonlinear spring abutments behavior.

Geometric nonlinearity through considering local (P-δ) and global (P-Δ) effects will be applied to this bridge in addition to material nonlinearity. The elasto-plastic behavior is modeled in two types : (1) distributed plasticity model, when it is modeled accounting for spread-of-plasticity effects in sections and along the beam-column element and (2) plastic hinge, when inelastic behavior is concentrated at plastic hinge locations. The proposed method can capture the spreading of plasticity along the members with computational efficiency and the necessary degree of accuracy, usually only one element per physical member is necessary to analyze. Therefore the nodes, in numerical model, can be placed only at the ends of physical members (Figure 1). The superstructure has been modeled with three elements per each span and the columns with three elements per each column and the work lines of the elements are located along the centroid of the superstructure.

In the concentrated plasticity model (plastic hinge approach), determination of the moment of inertia and torsional stiffness of the superstructure are based on uncraked cross sectional properties because the superstructure is expected to respond linearly to seismic loadings. The moment of inertia for columns will be calculated based on the cracked section using moment-curvature (M-Φ) curve. To accurately determine beam and column moment-curvature relationships, separate computer analyses using an element fibre model were conducted. A parabolic concrete stress-strain relationship and a linear elastic-perfectly-plastic relationship for the longitudinal reinforcement were used.

The total mass of the structure was lumped to the nodes of the superstructure (nodes 1,4,5,8,9,12 in Fig. 1). An additional load of 50 kN/m of superstructure was considered to represent loads from traffic barriers and wearing surface overlay.

The abutments have been modelled with a combination of full restraints (vertical translation and superstructure torsional rotation) and an equivalent spring stiffness (longitudinal and transverse translation), as shown in Figure 1. The stiffness of each abutment is represented by and equivalent spring stiffness with linear/nonlinear behavior. In the Table 1 are depicted the values for the equivalent spring stiffness of each abutment used in this analysis.

Table 1. Abutment spring stiffness

Longitudinal		Transversal	
K_{x1}	38400 kN/m	K_{z1}	14000 kN/m
K_{x2}	0 kN/m	K_{z2}	14000 kN/m
Yielded displacement	10 cm	-	

1.2 SEISMIC LOADING

To perform analysis of structure, the next step after modelling is applying loads. Design response spectrum should be available in order to perform NSP. Type I for elastic spectrum response and ground type A was assumed in analysis and a 5% damped response spectrum for every peak ground accelerations is assumed.

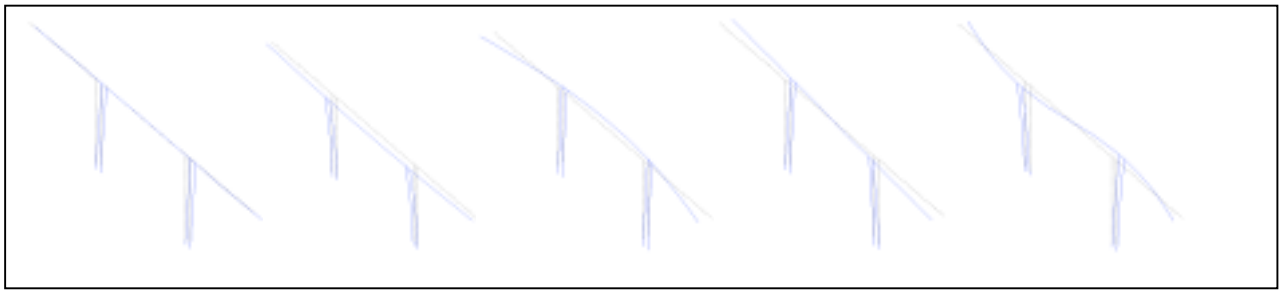

Mode 1 (T=1.135s) Mode 2 (T=0.882) Mode 3 (T=0.580) Mode 4 (T=0.794) Mode 5(T=0.366)

Figure 2. Modal analysis

Table2. Seismic loads

Mode 1-Longitudinal (T=1.13s) **Effective modal mass=99.8%** **Base shear force=8378 kN**	**Mode 1- Transversal (T=0.882s)** **Effective modal mass=99.4%** **Base shear force=10541 kN**
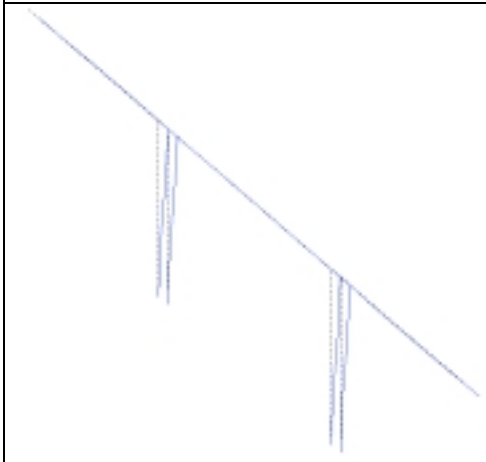	
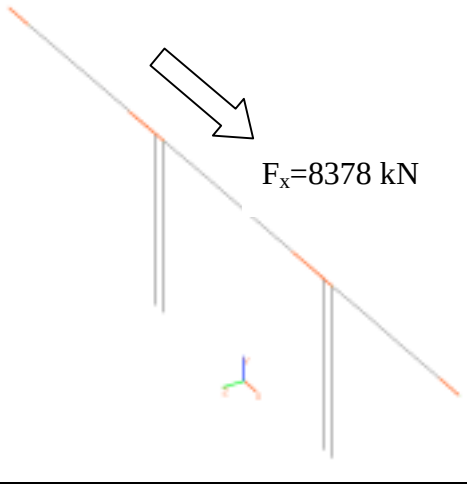	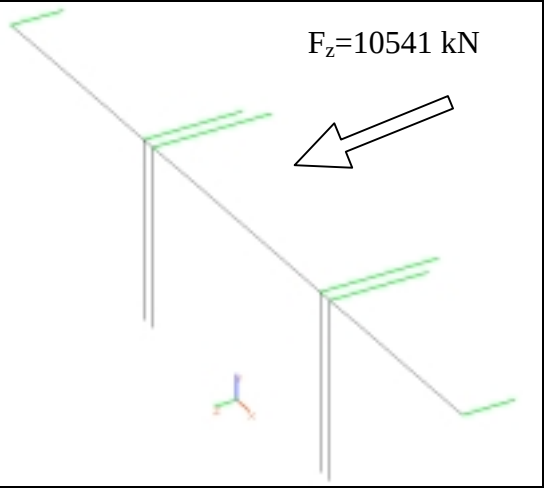

A 3D MDOF structural model is used in order to perform the modal analysis. Based on modal analysis and elastic response spectrum, the lateral force distribution corresponding to first mode in each direction was obtained and also the effective modal mass coefficients. Period of the first mode in transversal direction is 0.882

seconds and effective modal mass for this mode is 99.4%. The total base shear force corresponding at PGA=0.3g is 10541 kN (Table 2). Period of the first mode in the longitudinal direction is 1.135 seconds and effective modal mass is equal with 99.8% . The total base shear force corresponding at peak ground acceleration 0.3g is 8378 kN. The distribution of lateral loads for each case is also depicted in Table 2.

1.3. Inelastic analysis data

In addition to the data for the usual elastic analysis we need informations about nonlinear force deformations relationships for structural members. The plastic hinge analysis was performed using elastic perfect plastic force-generalized strain relationships, for each integration point generated along the member length. In the fiber approach the cross-section stiffness is modeled by explicit integration of stresses and strains over the cross-section area.
For plastic hinge analysis, an interaction surface for each cross-sectional type was developed through accurate fibre model analysis, and then this curves were interpolate using a cubic polynomial equation.

Fiber model

The concrete stress-strain relationship under compression is represented by a combination of a second-degree parabola (ascendant part) and a straight line (descendent part) as follows:

For $\varepsilon_c/\varepsilon_0 \leq 1$ (i.e., ascending curve)

$$f_c = \left(2 - \frac{y}{c}\frac{\varepsilon}{\varepsilon_0}\right)\frac{y}{c}\frac{\varepsilon}{\varepsilon_0} f''_c$$

and $\varepsilon_c/\varepsilon_0 > 1$ (i.e., descending curve)

$$f_c = \left[1 - \beta\left(\frac{y}{c}\frac{\varepsilon}{\varepsilon_0} - 1\right)\right] f''_c$$

where $\beta = \gamma\varepsilon_0/(\varepsilon_u - \varepsilon_0)$; and γ = degree of confinement of the concrete (usually taking as 0.15 for normal-weight concrete under normal loading conditions). This combination allows for the modeling of creep and confinement of the concrete simply by varying the parameters ε_0 and γ, respectively.

The stress-strain relationship of the conventional rebars is elastic-plastic and multilinear in both tension and in compression. The rebars' strain-hardening effects are not included.

Also, the strain in the prestressing tendons at any level is equal to the strain in the surrounding concrete plus the strain difference $\Delta\varepsilon p$ (i.e., the initial strain imposed to the prestressed steel during its tensioning) at this level; thus

$$\varepsilon_{pf} = \varepsilon_c + \Delta\varepsilon_p$$

The stress-strain relationship of the prestressed steel is expressed by a Ramberg-Osgood function as follows:

$$f_p = E_p \varepsilon_{pf} \left\{ A^* + \frac{1 - A^*}{[1 + (B^* \varepsilon_{pf})^e]^{1/e}} \right\}$$

where *A**, *B**, and *e* are parameters found from a material tensile test. For low-relaxation strands with *fpu* = 1,860 MPa (270 ksi), an appropriate formulation is

$$f_p = E_p \varepsilon_{pf} \left\{ 0.025 + \frac{0.975}{[1 + (118 \varepsilon_{pf})^{10}]^{0.10}} \right\}$$

Plastic hinge model

In the plastic hinge approach, the values of the bending axial, and torsional capacities of a member are dependent upon the interaction among the internal forces at the cross section. For beam-column elements, the yielding surface is based on the nonlinear interactions and the von Mises yield criterion.

The interaction relations between the biaxial bending and the axial force were employed in this study. The interaction equation used in the computational example is:

$$\left(\frac{M_y}{M_{py}} \right)^{\alpha} + \left(\frac{M_z}{M_{pz}} \right)^{\alpha} = 1$$

in which M_y and M_z are the applied moments about the minor and major axes respectively and M_{py} and M_{pz} are the modified plastic moments that include the effect of the axial compressive force, N. The plastic moments are evaluated approximately using a cubic polynomial interpolation curve based an exact interaction curves obtained through an accurate fiber model. The exponent α is a numerical factor whose value depends on the shape of a particular cross-section and the magnitude of the axial load. A constant value α=1.6 was used in this study.

The procedures for reducing the plastic capacities are as follows: At any time step in the structural analysis, a reduction of plastic moments M_{py} and M_{pz} must be made to include the influence of the compressive axial force based on interpolation curve. These modified plastic moments, must then be reduced because of the torsional effect in amount of $\sqrt{1-\left(\frac{M_x}{M_{px}} \right)^2}$. The torsional influence should also be applied to the axial force to change its capacity. The final reduced plastic moments and the axial force is employed in the stiffness coefficients for the next step in the analysis.

Computed member properties for both beams and column sections using the fiber model analysis are summarized in Table 3 and Figures 3-5 respectively. The axial force-moment interaction diagram for relevant cross-sections, obtained by a fiber model analysis of the section is shown in figures 3.1, 4.1, 5.1. Also using the PM interaction loading along with failure material strains the variation of ultimate curvature vs. axial load is presented (Figures 3.2, 4.2, 5.2).

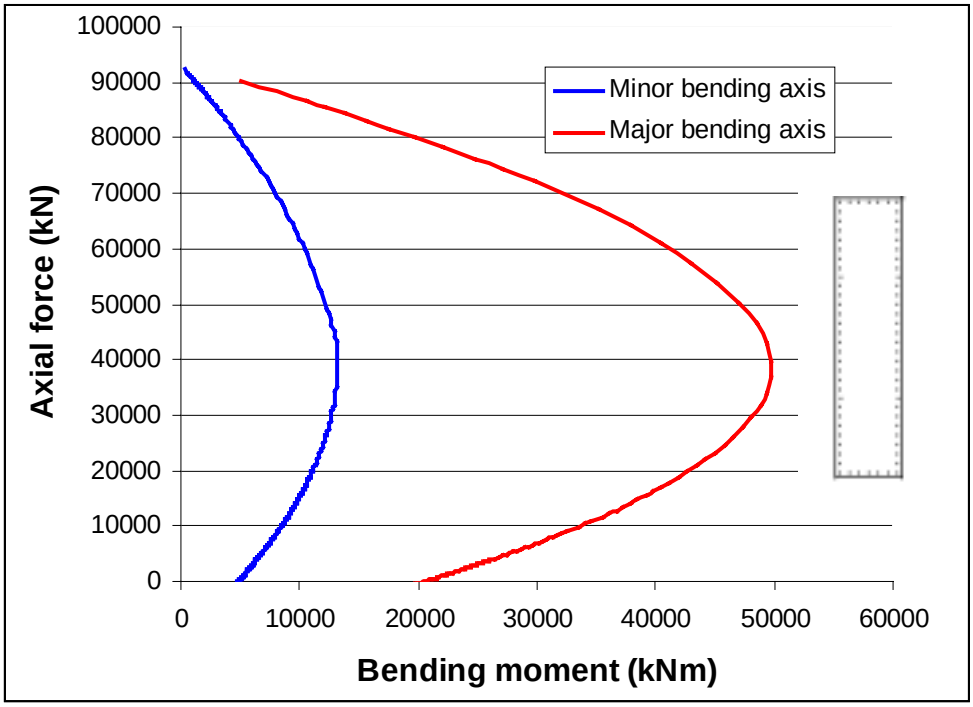

Figure 3.1. Interaction diagrams for column cross-section

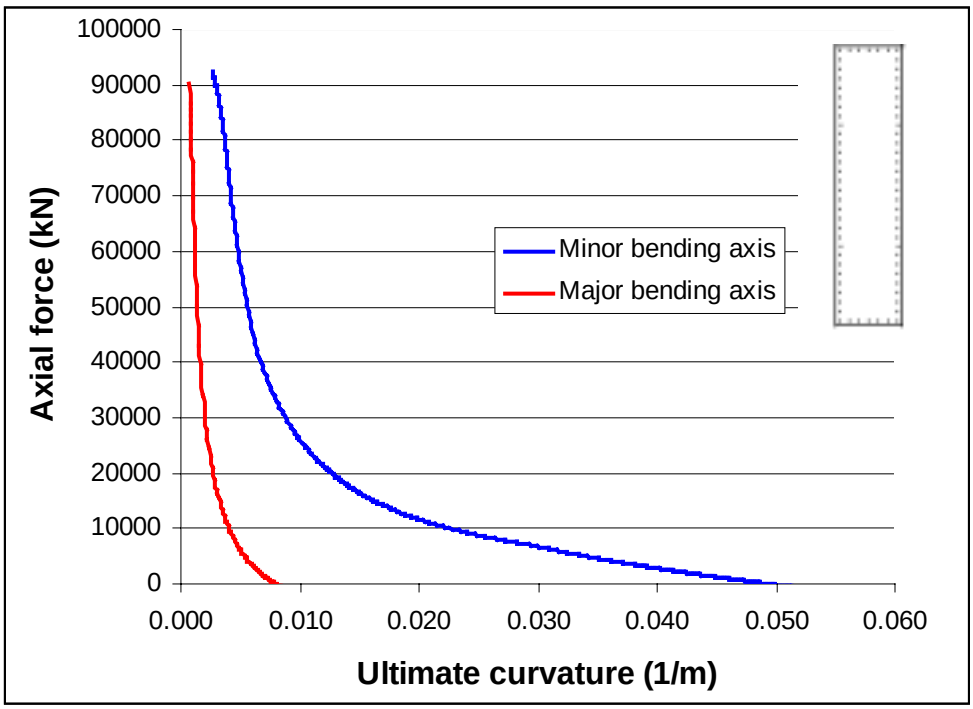

Figure 3.2. Axial force vs. ultimate curvature

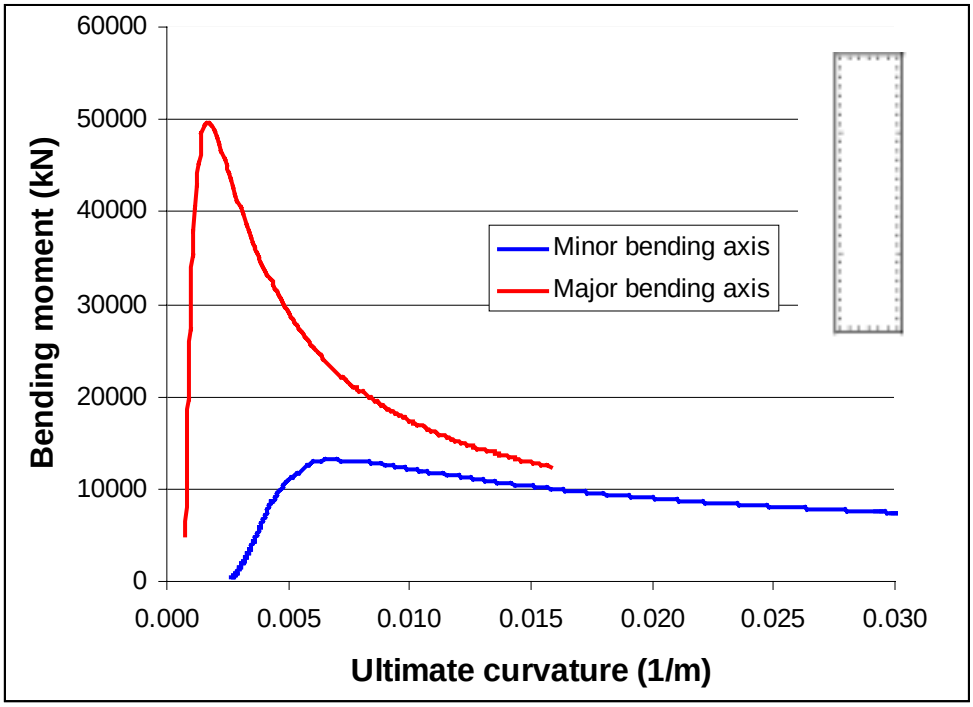

Figure 3.3. Bending moment vs. ultimate curvature

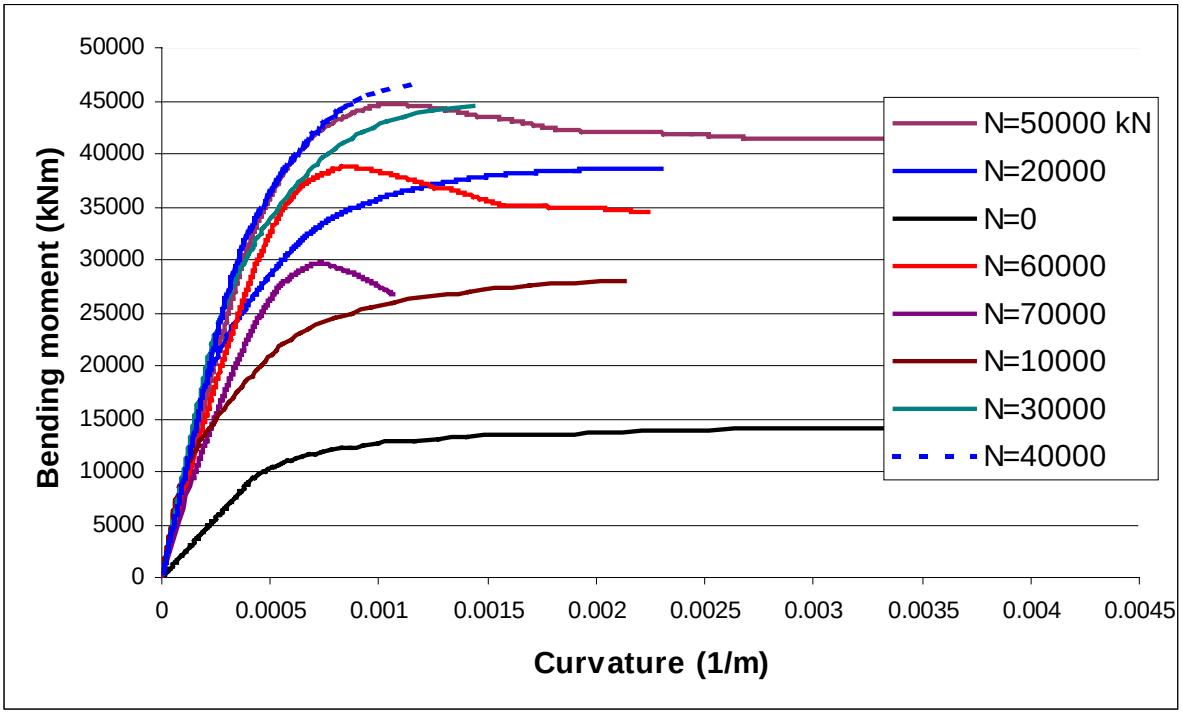

Figure 3.4. Effect of axial force on flexural rigidity (major axis bending)

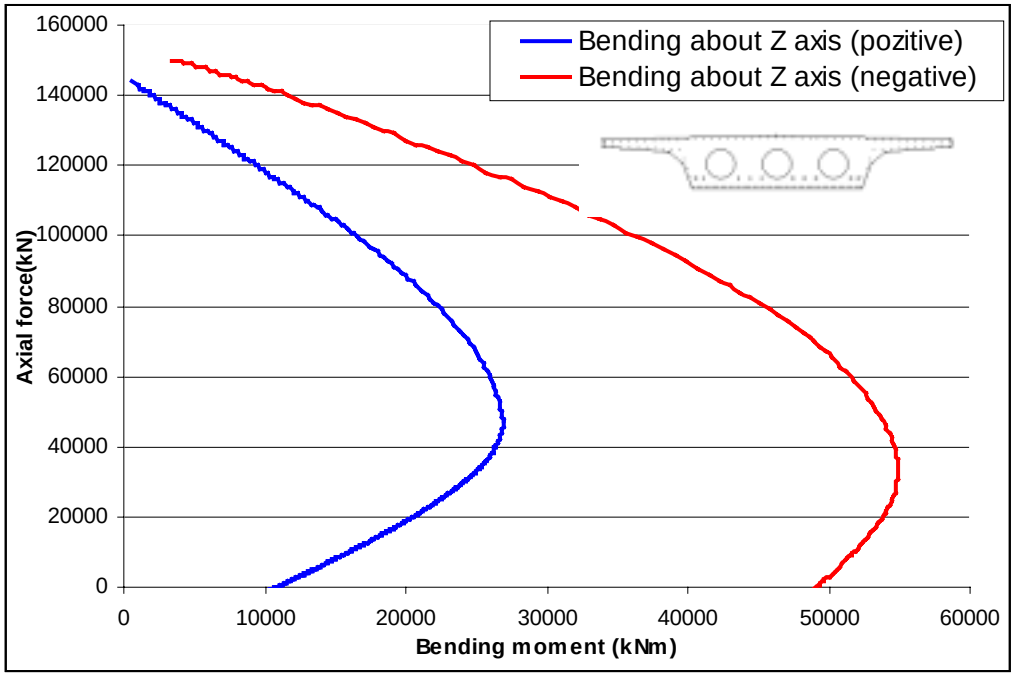

Figure 4.1. Interaction diagrams for deck cross-section

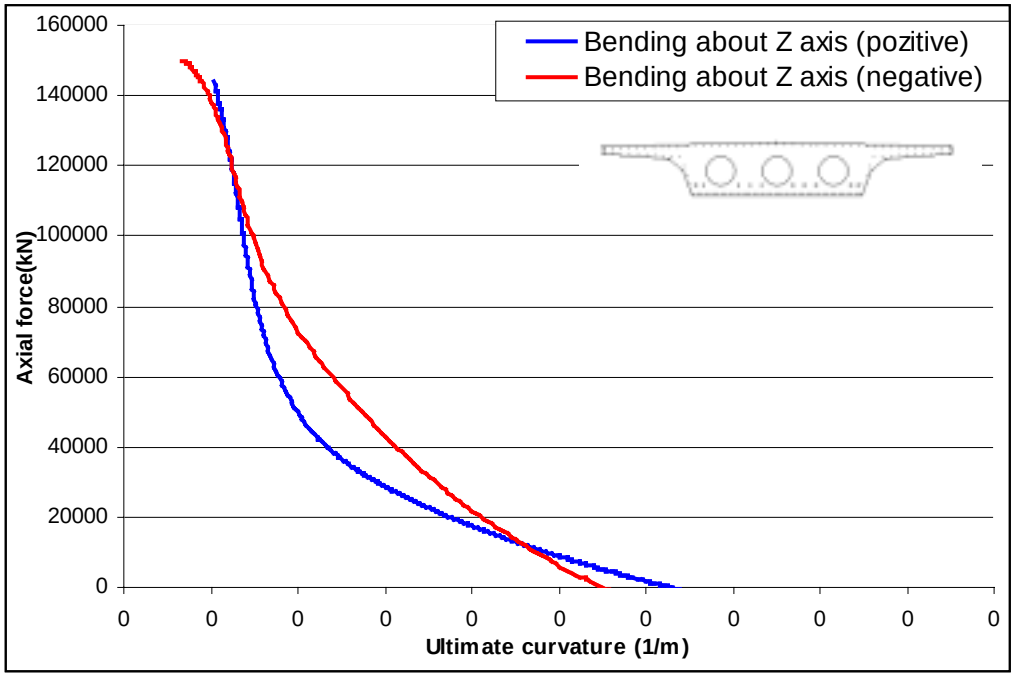

Figure 4.2. Axial force vs. ultimate curvature

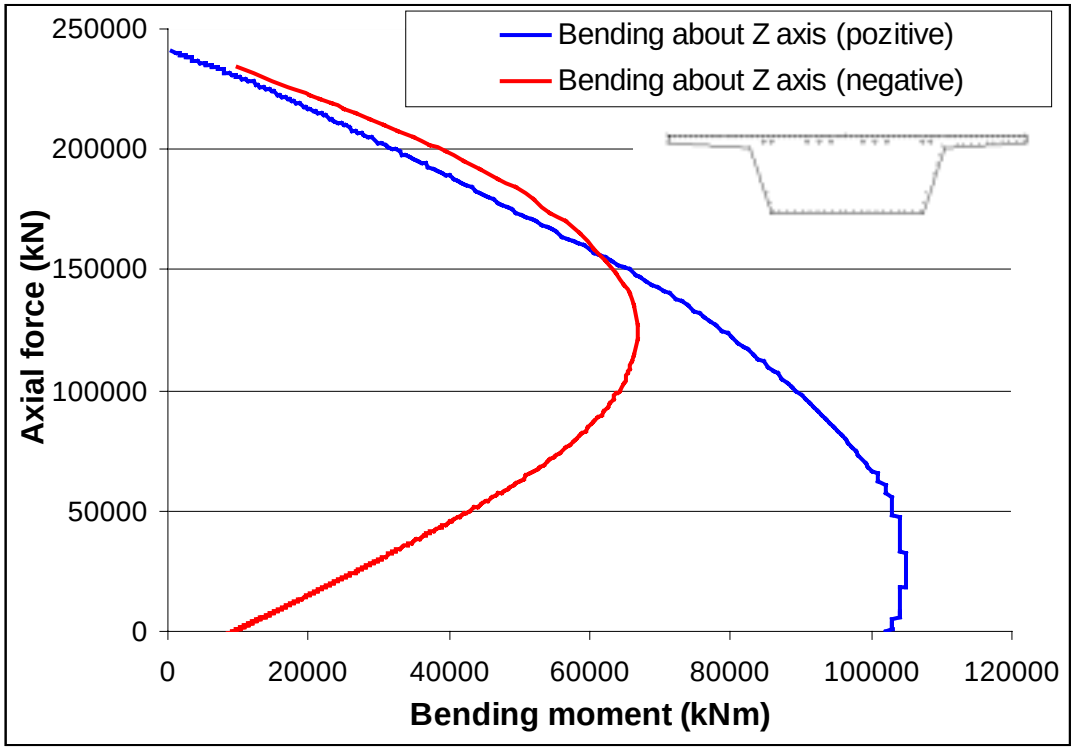

Figure 5.1. Interaction diagrams for deck cross-section

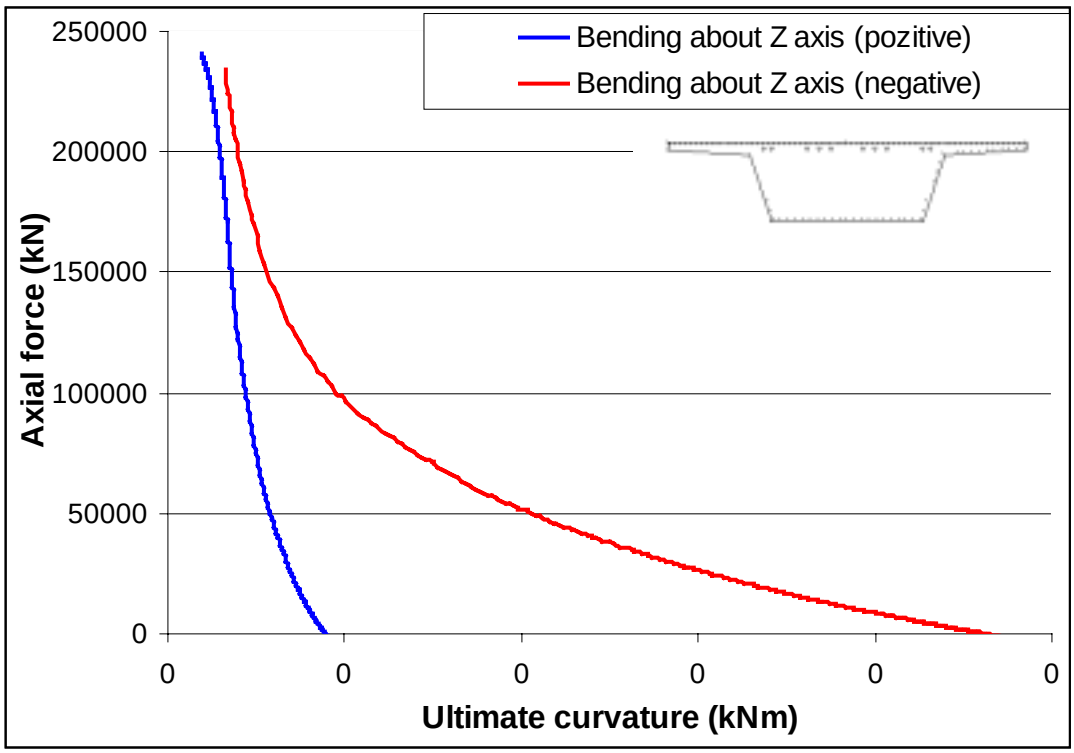

Figure 5.2. Axial force vs. ultimate curvature

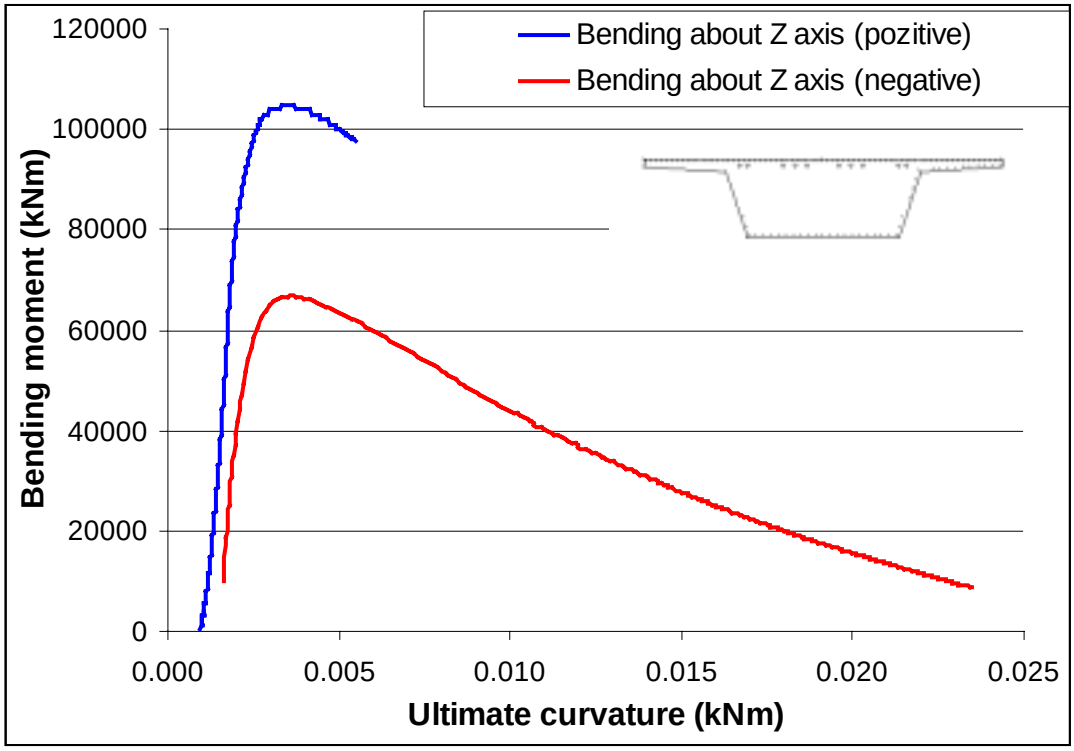

Figure 5.3. Bending moment vs. ultimate curvature

Table 3. Geometric characteristics of cross-sections

Superstructure		**Columns**	
	A=63703.84 cm^2 I_x=219733693 cm^4 I_y=2676376413 cm^4 I_z=114599919.8 cm^4	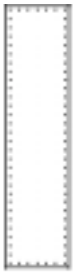	A=34199.98 cm^2 I_x=72862819 cm^4 I_y=23084988.46 cm^4 I_z=411539934.3cm^4
	A=76648.96 cm^2 I_x=219733693 cm^4 I_y=2676376413 cm^4 I_z=114096688.4cm^4		
	A=99419.95 cm^2 I_x=661267775 cm^4 I_y=2750710497 cm^4 I_z=357377364.1 cm^4		

2. RESULTS AND PARAMETRIC STUDY

A computational efficient 3D RC fiber beam column element was developed and implemented in the existing computer program NEFCAD [7]. This program was used in this study to perform the pushover analysis on a reinforced concrete bridge. The analysis includes the second order effects in addition to material nonlinearity and nonlinear spring stiffness abutments behavior. Nonlinear beam-column elements, which consider spread of plasticity along the element length were used to model the

beam and the columns of the structure. The integration along the element was based on the Gauss-Lobatto quadrature rule with 5 points of integration along the element length. Analysis of the bridge consisted of first performing a gravity and prestressed load analysis on the model. Then, a lateral load pattern with linear time series was applied to the bridge to the bridge. The gravity loads was modeled as a uniform distributed loads along the superstructure length and the prestressed axial forces was included in the beam-columns elements of the superstructure.

Arc length control was used for whole pushover analysis using the predefined load pattern shown in Table 2. The lateral loads were incrementally increased until the collapse mechanism occurs. The control point was monitorized for each increment of the analysis.

Analyses were performed for two levels of seismic load intensity. For the first level (Design Level), PGA = 0.3g and for the second level (Maximum Considered Earthquake, MCE, Level), PGA = 0.6g. Different performance objectives are checking for the maximum displacement, total base shear, and rotation of plastic hinges/curvatures resulting from the NSP.

2.1 Longitudinal direction

Pushover curve for this direction obtained in a fiber analysis model and idealized pushover curve are shown in Figure 6. Comparable load displacement curves for both fiber and plastic hinge approach are also depicted in Figure 7. The ultimate load factor obtained in “fiber” model is 1.19 corresponding to a total base shear force (yield force) equal with 9970 kN. The initial stiffness of the idealized system is determined in such way that the areas under the actual and the idealized force-deformation curves are equal. A bilinear idealization of the pushover curve is shown in Figure 6. The yield strength and displacement amount to F_y =9970 kN and D_y=13.70 cm. The estimated target displacement is 9.9 cm for the design level (PGA=0.3g) and 20.2 cm for the MCE level (PGA=0.6g).

In a plastic hinge analysis the inelastic limit point is 1.24 that correspond to a total base shear force equal with 10388 kN.

Expected performance can assessed by comparing the seismic demands with the capacities for the relevant performance level. Global performance can be visualized also by comparing displacement capacity and demand (Figure 6).

Table 4 summarize different parameters used in this study for seismic performance evaluation: distribution of plastic zones along the member length with percentage of sections area yielded, distribution of flexural rigidities, deflected shapes and plastic status for most critical sections.

Longitudinal direction

Table 4. Summarized global and local seismic demands.

PGA=0.3g **Applied load factor=1.03**	**PGA=0.6g** **Applied load factor=1.11**	**Collapse** **Ultimate load factor=1.19**
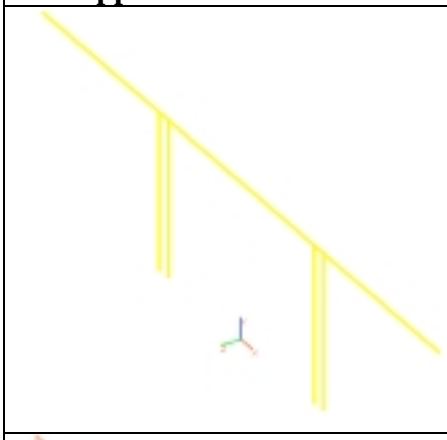	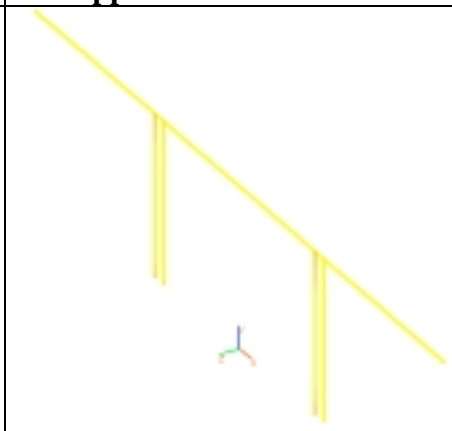	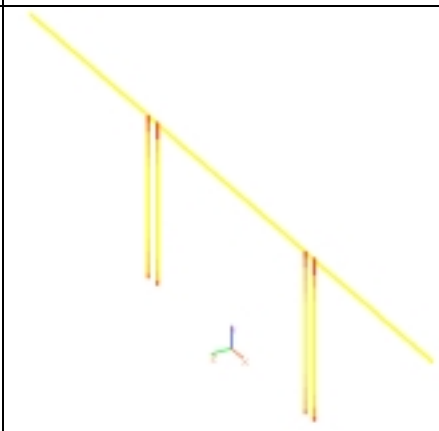
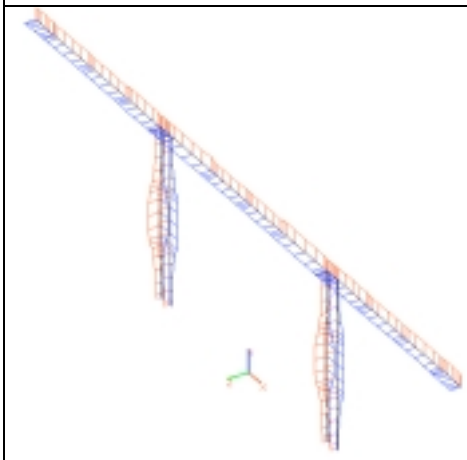	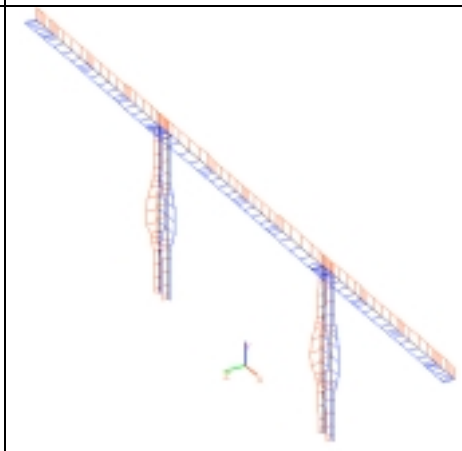	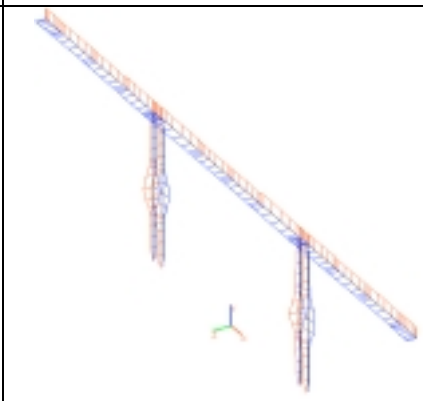
D_u=50 cm	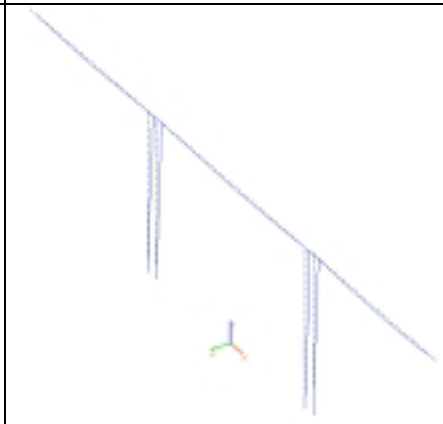	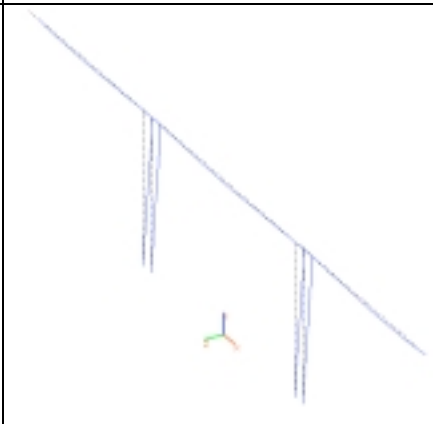
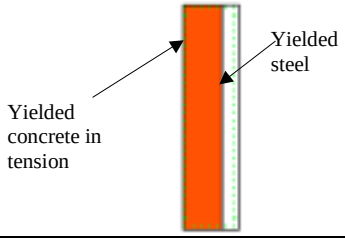		

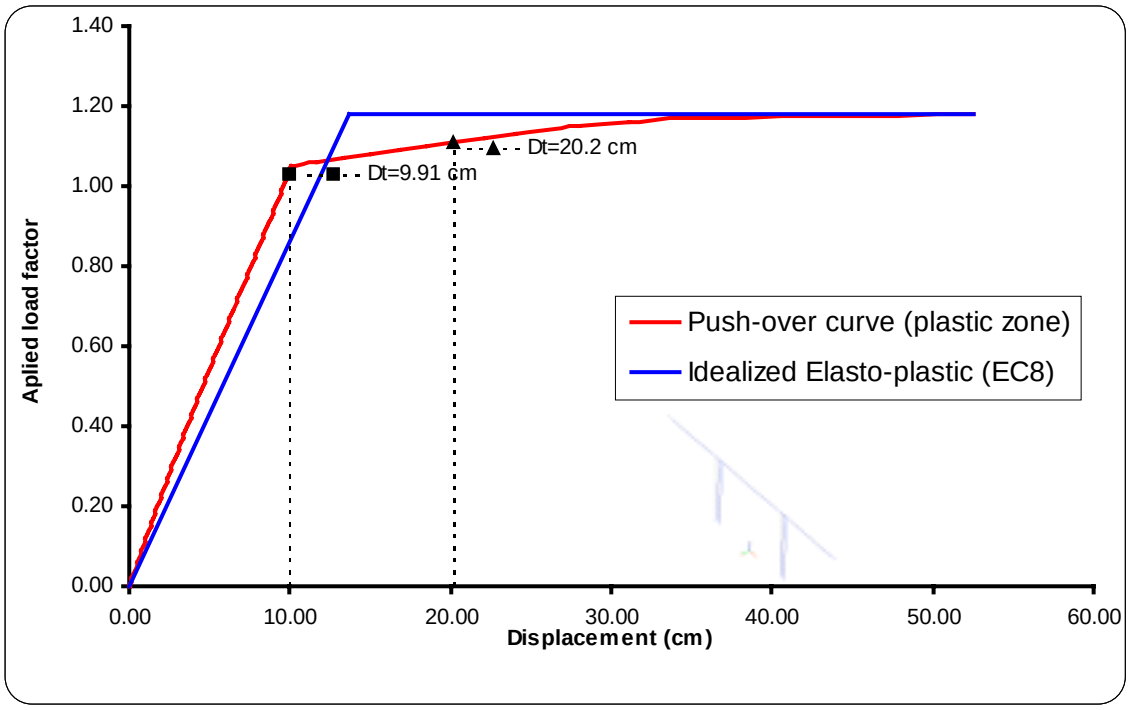

Figure 6. Pushover curve and corresponding capacity diagram (longitudinal direction).

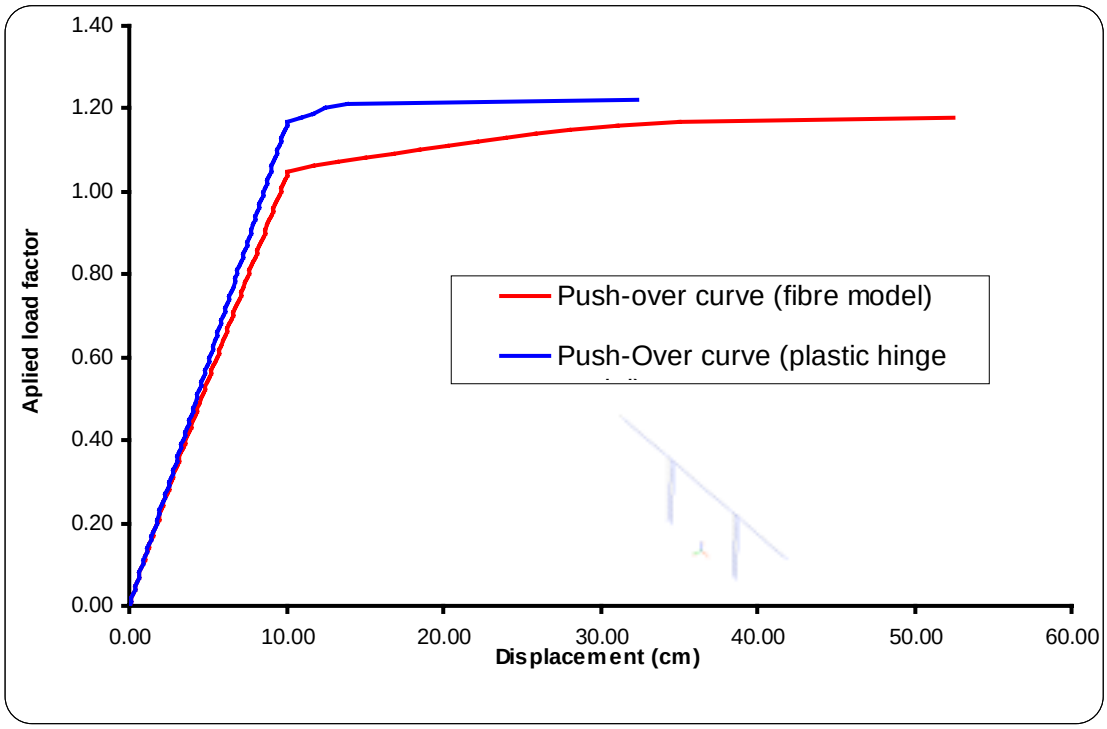

Figure 7. Pushover curves (longitudinal direction). Fibre vs plastic hinge approach.

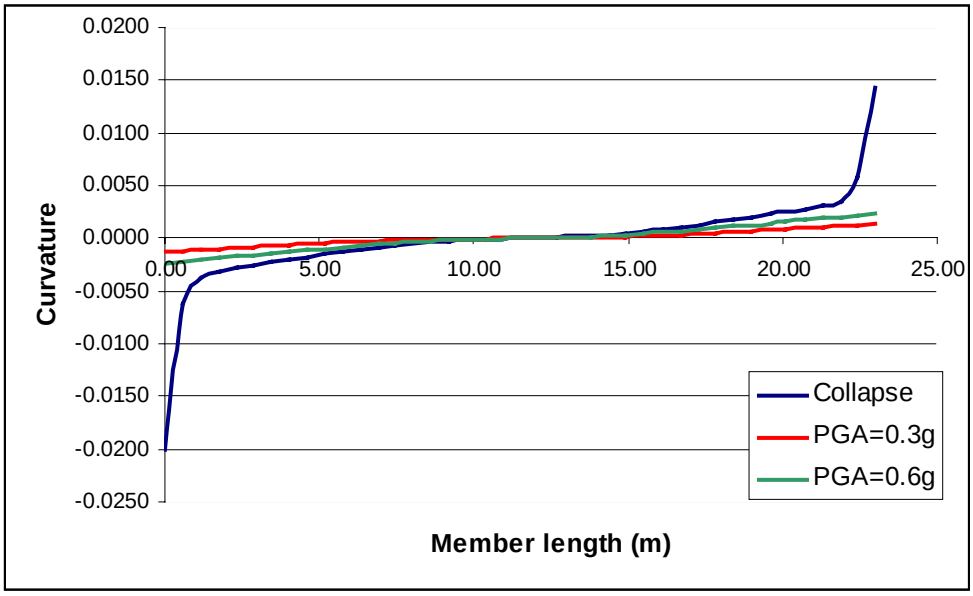

Figure 8. Local seismic demands. Variation of curvature along the column length

2.2. Transversal direction

Pushover curve for this direction obtained in a fiber analysis model and idealized pushover curve are shown in Figure 9. Comparable load displacement curves for both fiber and plastic hinge approach are also depicted in Figure 10. The ultimate load factor obtained in "fiber" model is 1.71 corresponding to a total base shear force (yield force) equal with 18025 kN. The initial stiffness of the idealized system is determined in such way that the areas under the actual and the idealized force-deformation curves are equal. A bilinear idealization of the pushover curve is shown in Figure 9. The yield strength and displacement amount to F_y =18025 kN and D_y= 48.3 cm. The estimated target displacement is 8.1 cm for the design level (PGA=0.3g) and 29 cm for the MCE level (PGA=0.6g).

In a plastic hinge analysis the inelastic limit point is 1.65 that correspond to a total base shear force equal with 17392 kN.

Expected performance can assessed by comparing the seismic demands with the capacities for the relevant performance level. Global performance can be visualized also by comparing displacement capacity and demand (Figure 9).

Table 5 summarize different parameters used in this study for seismic performance evaluation: distribution of plastic zones along the member length with percentage of sections area yielded, distribution of flexural rigidities, deflected shapes and plastic status for most critical sections.

Transversal direction

Table 5. Summarized global and local seismic demands.

PGA=0.3g **Applied load factor=0.53**	**PGA=0.6g** **Applied load factor=1.16**	**Collapse** **Ultimate load factor=1.71**
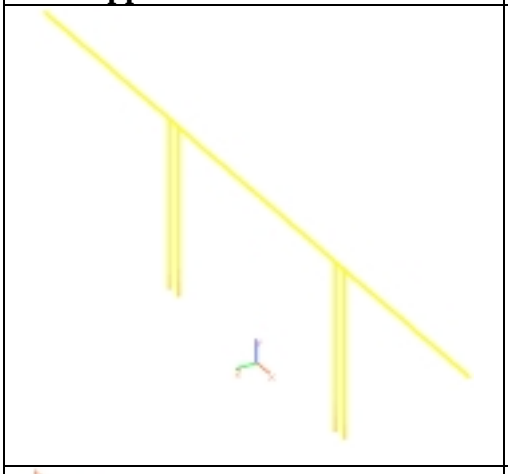	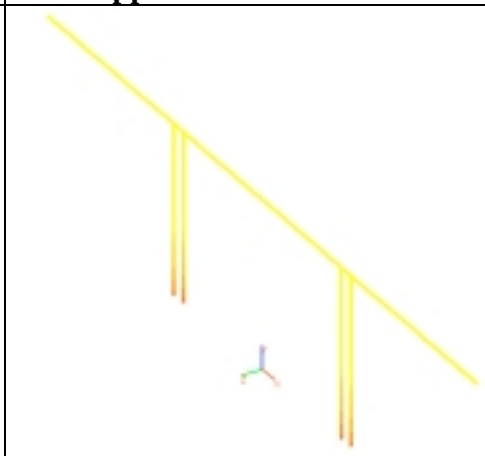	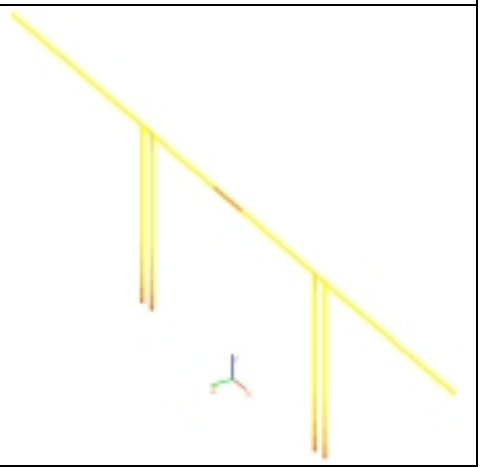
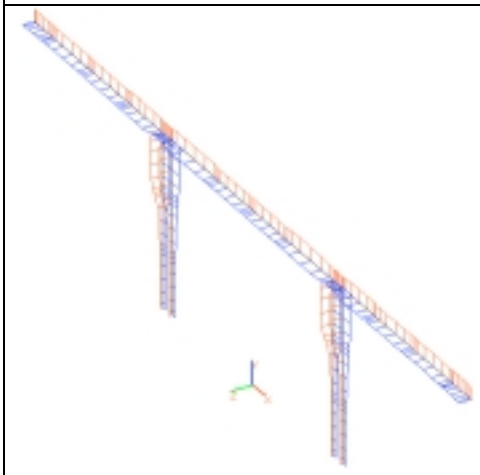	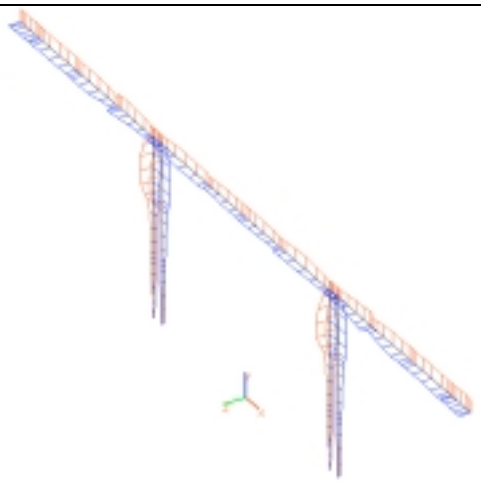	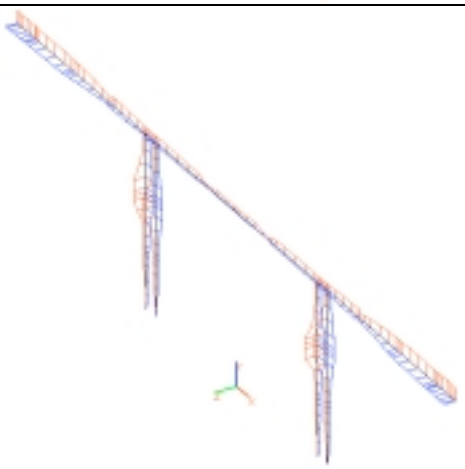
D_t=90 cm		
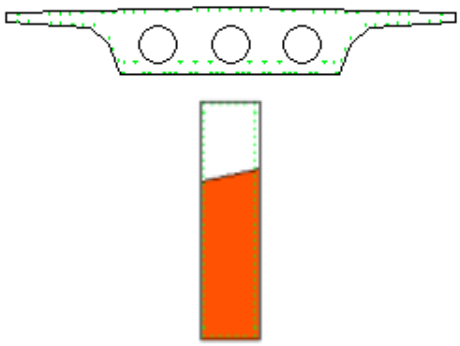	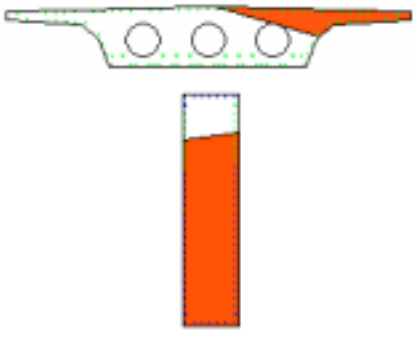	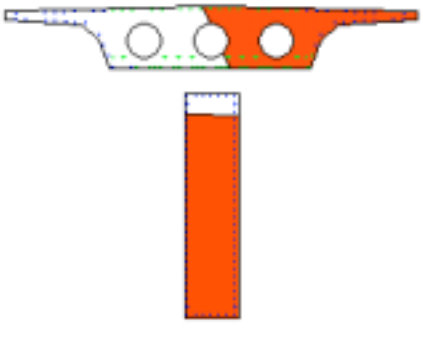

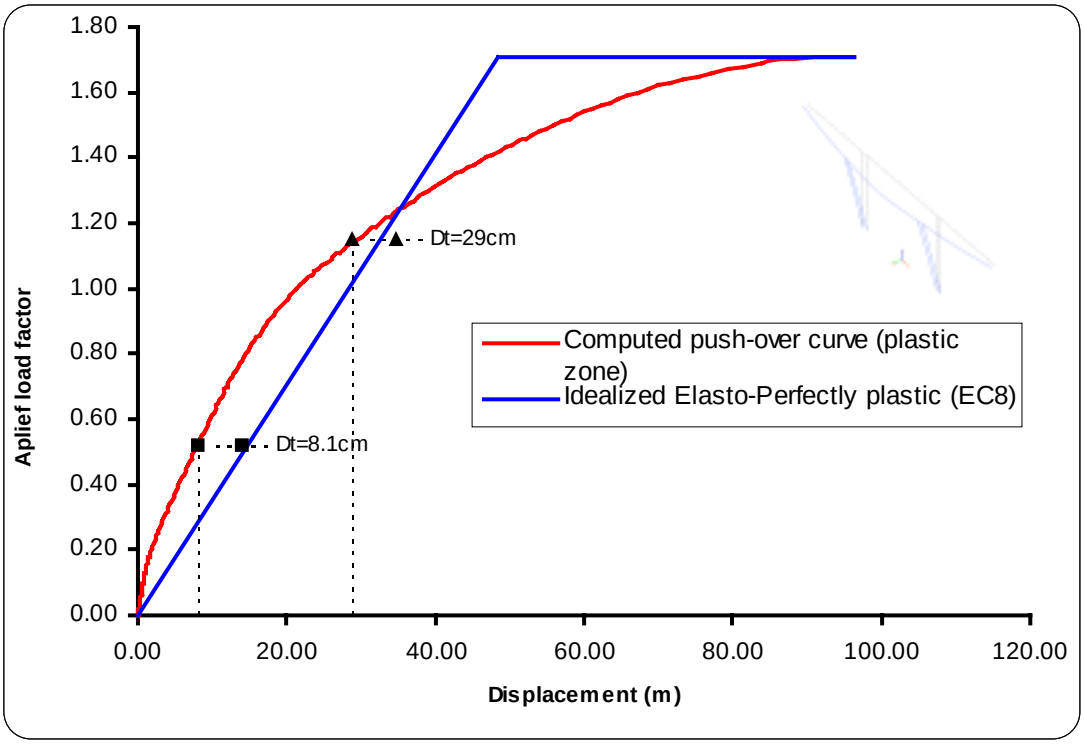

Figure 9. Pushover curve and corresponding capacity diagram (transversal direction).

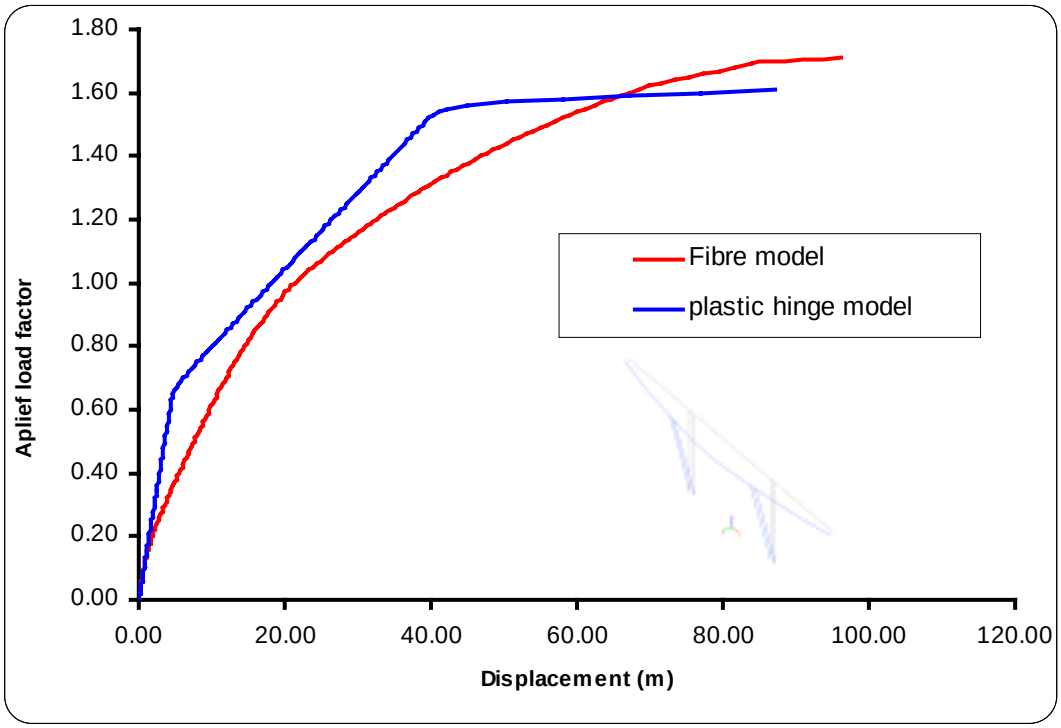

Figure 10. Pushover curves (transversal direction). Fibre vs plastic hinge approach.

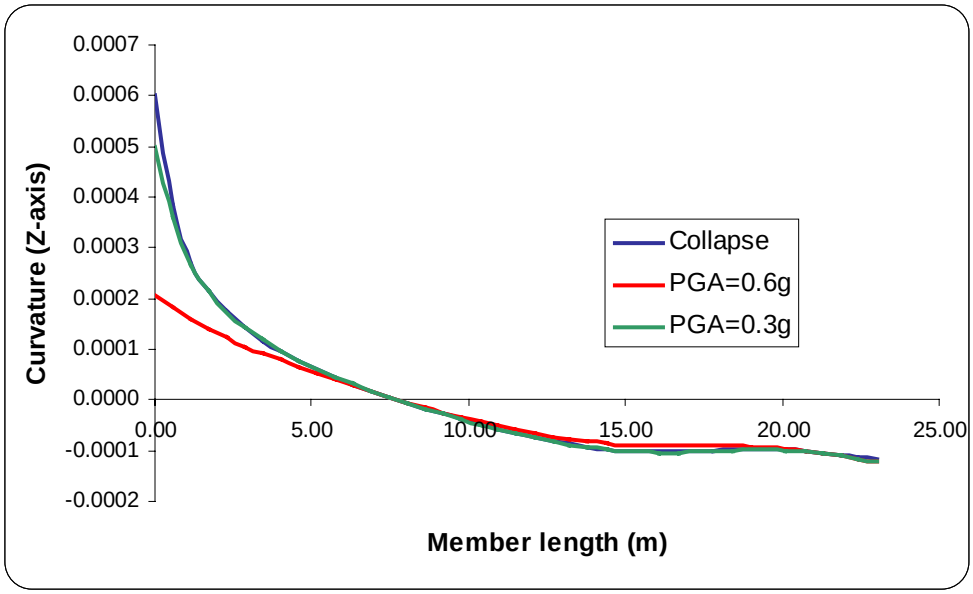

Figure 11. Local seismic demands. Variation of curvature along the column length

3. SUMMARY AND COCLUDING REMARKS

This report presents partial results of a POCTI/36019/99 initiation research project for studying the response behavior of inelastic bridge system subjected to static loads.

A computational efficient 3D RC fiber beam column element was developed and implemented in a nonlinear inelastic analysis computer program. The 3D RC fiber beam column element allowing for the formation of plastic zones along the member is derived in terms of flexibility based approach [7]. The effects of distributed plasticity, distributed loads, uniform or nonuniform members, variation of reinforcing bars along the member can be captured using only one element/physical member with sufficient accuracy and less computational effort.

The nonlinear inelastic analysis carried out includes the second order effects in addition to material nonlinearity. The proposed analysis can practically account for all key factors influencing 3D RC frame behavior: gradual yielding associated with biaxial bending and axial force, shear and torsional deformations, local and global second order effects with computational efficiency.

The nonlinear pushover analysis, or collapse mode analysis, is a simple and efficient technique to study the response of a building. The pushover analysis is carried out by incrementally applying lateral loads, or displacements to the structure. The sequence of component cracking, yielding, and failure, as well as the history of deformations and shears in the structure, can be traced as the lateral loads (or displacements) are monotonically increased. Furthermore, strength and service limit states, such as the failure of an element, the formation of a collapse mechanism, etc., can be identified.

Applicability of the non-linear static procedure, described here, to seismic performance evaluation of bridges is investigated in this study using the capacity spectrum method, which was presented by EC8 (2003). A three span bridge was presented and described as a case study.

Load deflection curves, target displacements, base shear and deformation of plastic zones (hinges) obtained from this procedure was presented and will be compared with the corresponding values resulting from the more accurate but more time consumption, nonlinear time history analysis, in framework of a future work.

Separate analyses of the soil-foundation and the abutment systems, are underway to establish the real equivalent spring properties to be used at the base of the piers and at the abutments supports.

Pushover analysis can provide good estimates of global and local inelastic deformations demands and it will also expose the design weaknesses that may remain hidden in an elastic analysis. However, pushover analysis has its limitations because it is based on a static loading, so it cannot represent dynamic phenomena as well as a nonlinear dynamic analysis. A fundamental assumption made for pushover analysis is that first mode dominates, and that the higher mode effects are not significant. To follow more closely the time variant distributions of inertial forces the adaptive force distribution or modal pushover analysis procedure can be applied.

4. REFERENCES

1. Chopra, A.K. and Goel, R.K. (2001). *A Modal Pushover Analysis Procedure to Estimate Seismic Demands for Buildings: Theory and Preliminary Evaluation*. *Tech. Rep.2001/3,* Pacific Earthquake Engineering Research Center, University of California, Berkeley, CA.

2. Federal Emergency Management Agency (FEMA) (1997). *NEHRP Guidelines for the Seismic Rehabilitation of Buildings. FEMA-273*, Washington, D.C.

3. Federal Emergency Management Agency (FEMA) (1997). "*NEHRP recommended Provisions for Seismic Regulations for New Buildings and Other Structures*." *FEMA-302*, Washington, D.C.

4. Applied Technology Council (ATC). (1996). "*Seismic Evaluation and Retrofit of Concrete Buildings*." *Rep. No. SSC 96-01: ATC-40, 1,* Redwood City, Calif.

5. Gupta, A., Kunnath, S.K., *Adaptive Spectra-based Pushover Procedure for Seismic Evaluation of Structures*, Eartquake Spectra, 16, 367-392.

6. Chiorean, C.G., *Contributions to advanced analysis of Frame Structures*, PhD Thesis, Technical Univ. of Cluj, 2000.

7. Chiorean C.G., *Application of pushover analysis on reinforced concrete bridge model, Part I-Numerical models*, Research report, UNL/FCT-DEC,2003

8. Eurocode 8, *Design of structures for earthquake resistance*, January, 2003, European Committee for Standardization, 2000.